HHS Public Access

Author manuscript

J Am Soc Echocardiogr. Author manuscript; available in PMC 2021 August 01.

Published in final edited form as:

J Am Soc Echocardiogr. 2020 August ; 33(8): 1023–1031.e2. doi:10.1016/j.echo.2020.03.016.

FLOW AUGMENTATION IN THE MYOCARDIUM BY ULTRASOUND CAVITATION OF MICROBUBBLES: ROLE OF SHEAR-MEDIATED PURINERGIC SIGNALING

Federico Moccetti, M.D.[a,b], **Todd Belcik, M.S.**[a], **Yllka Latifi, M.D.**[a], **Aris Xie, M.S.**[a], **Koya Ozawa, M.D., Ph.D.**[a], **Eran Brown, B.S.**[a], **Brian P. Davidson, M.D.**[a], **William Packwood, B.S.**[a], **Azzdine Ammi, Ph.D**[a], **Sabine Huke, Ph.D.**[c], **Jonathan R. Lindner, M.D.**[a,d]

[a]Knight Cardiovascular Institute, Oregon Health & Science University, Portland, Oregon; [b]Cardiology Department, Heart Centre Lucerne, Lucerne, Switzerland; [c]Division of Cardiovascular Disease, University of Alabama at Birmingham, Birmingham, Alabama. Dr. Sabine Huke passed away in 2018. [d]Oregon National Primate Research Center, Oregon Health & Science University, Portland, Oregon;

Abstract

Background: Ultrasound-mediated cavitation of microbubble contrast agents produces high intravascular shear. We hypothesized that microbubble cavitation increases myocardial microvascular perfusion through shear-dependent purinergic pathways downstream from ATP release that is immediate and sustained through cellular ATP channels such as Pannexin-1.

Methods: Quantitative myocardial contrast echocardiography (MCE) perfusion imaging and *in vivo* optical imaging of ATP was performed in wild-type and Pannexin-1-deficient ($Panx1^{-/-}$) mice before, 5 and 30 minutes after 10 minutes of ultrasound-mediated (1.3 MHz, mechanical index 1.3) myocardial microbubble cavitation. Flow augmentation in a pre-clinical model closer to humans was evaluated in rhesus macaques undergoing MCE perfusion imaging after high-power cavitation in the apical 4-chamber plane for 10 minutes.

Results: Microbubble cavitation in wild-type mice (n=7) increased myocardial perfusion by 64±25% at 5 minutes and 95±55% at 30 minutes compared to baseline ($p<0.05$). In $Panx1^{-/-}$ mice (n=5), perfusion increased by 28±26% at 5 minutes ($p=0.04$) but returned to baseline at 30 minutes. Myocardial ATP signal in wild-type (n=7) mice undergoing cavitation compared to sham-treated controls (n=3) was 450-fold higher at 5 min and 90-fold higher at 30 minutes after cavitation ($p<0.001$). ATP signal in $Panx1^{-/-}$ mice (n=4) was consistently 10-fold lower than wild-type mice and was similar to sham controls at 30 minutes. In macaques (n=8), myocardial

Address correspondence to: Jonathan R. Lindner, MD, Knight Cardiovascular Institute, UHN-62, Oregon Health & Science University, 3181 SW Sam Jackson Park Rd., Portland, OR 97239, Tel. (503) 494-3574, Fax. (503) 494-8550, lindnerj@ohsu.edu.

perfusion increased 2-fold in cavitation-exposed 4-chamber plane, similar in degree to that produced by adenosine, but did not increase in the control 2-chamber plane.

Conclusions: Cavitation of microbubbles in the myocardial microcirculation produces an immediate release of ATP, likely from cell microporation, and sustained release which is channel dependent and responsible for persistent flow augmentation. These findings provide mechanistic insight by which cavitation improves perfusion and reduces infarct size in patients with myocardial infarction.

Keywords

Contrast Ultrasound; Myocardial Blood Flow

In the working ventricular myocardium, perfusion is tightly regulated to meet myocardial metabolic requirements.[1] Multiple pathways act in parallel to produce vasodilation in response to increasing myocardial work or tissue ischemia.[2,3] Shear-dependent vasodilation is an evolutionarily-conserved mechanism to ensure that microvascular resistance does not limit appropriate flow response to metabolic demand.[2] Flow-mediated vasodilation is mediated, in part, through shear-dependent release of ATP from both endothelial cells and from red blood cells (RBCs) which produces not only immediate vasodilation, but also sustained vasodilation through activation of mechanosensitive channels such as Pannexin-1 (Panx1) and Piezo-1.[3–7]

Ultrasound (US) at a wide range of frequencies and acoustic pressures produces vasodilation.[8–10] This response is thought to involve shear produced by convective motion.[9] Ultrasound-mediated vasodilation and augmentation of tissue perfusion is markedly augmented by the presence of conventional microbubble (MB) contrast agents that undergo inertial cavitation at high acoustic pressures.[10] In skeletal muscle, MB cavitation at US frequencies and pressures in the diagnostic range increases tissue perfusion several fold in mice and in humans, and can reverse tissue ischemia.[10,11] Cavitation-mediated flow augmentation occurs largely through shear-mediated release of ATP with downstream signaling through endothelial nitric oxide (NO) and prostaglandins, and conversion of ATP to adenosine.[11] Release of ATP can be immediate from transient microporation of cells, and sustained for >24 hours, possibly reflecting purine channel activation.[11]

Inertial cavitation of MBs in the myocardial microcirculation in animal models and patients with myocardial infarction reduces infarct size, part from enhanced thrombolysis.[12,13] However, it is likely that some beneficial effects could have occurred from direct vasodilation. Little is known regarding the mechanism of coronary microvascular responses to cavitation other than the involvement of NO.[14] We hypothesized that MB cavitation in the coronary microcirculation triggers ATP release through established shear-sensitive pathways with myocardial flow augmentation occurring as a result of downstream purinergic signaling, similar to what has been seen in murine hindlimb models.[11] To test our hypothesis, ATP release and myocardial blood flow were temporally assessed after MB cavitation during myocardial contrast echocardiography (MCE) in mice, including those deficient for the shear-activated ATP channel Panx-1. Cavitation-mediated flow augmentation was also assessed in non-human primates (NHPs) undergoing MCE using

acoustic pressures and MBs approved for clinical use in order to better predict coronary microvascular responses expected in humans.

METHODS

Animal Models

The study was approved by the Animal Care and Use Committee of Oregon Health & Science University. Wild-type C57Bl/6 mice and mice deficient for Panx-1 (Panx1$^{-/-}$) were studied at 18–25 weeks of age. Mice were anesthetized with 1.0 to 1.5 % inhaled isofluorane and kept euthermic. The jugular vein was cannulated with a fluid-filled polyethylene catheter for intravenous administration of agents. Adult lean male rhesus macaques (*Macaca mulatta*) had induction anesthesia with Ketamine HCl (10 mg/Kg IM). An endotracheal tube was placed and anesthesia was maintained using 1.0 to 2.0 % inhaled isoflurane. Continuous heart rate by electrocardiogram, pulse oximetry and capnography were performed; and arm cuff blood pressure was monitored every 3–5 minutes.

Microbubble Preparation

For murine studies, lipid-shelled decafluorobutane MB were prepared as previously described.[11] Briefly, MB were formed by sonication of a decafluorobutane -saturated aqueous solution containing distearoylphosphatidylcholine (2 mg/mL) and of distearoylphosphatidylethanolamine-PEG(2000) (1 mg/mL). Microbubble concentration and size distribution were measured with electrozone sensing (Multisizer III, Beckman Coulter). For NHP studies a commercially-available perflutren contrast agent (Definity, Lantheus Medical Imaging, N. Billerica, MA) was activated prior to use.

Therapeutic Cavitation Protocols

The experimental protocols for mice and rhesus macaques is illustrated schematically in Figure 1. For cavitation in mice, a phased-array transducer interfaced with an US system (SONOS 7500, Philips Ultrasound, Andover, MA) was positioned over the chest in a parasternal short-axis orientation. Imaging was performed at the mid-ventricular level, the position for which was guided by placing a wire for spatial registration under high-frequency (30 MHz) echocardiography (Vevo 2100, VisualSonics, Toronto, Canada). For cavitation, US was transmitted at a carrier frequency of 1.3 MHz using multi-pulse harmonic Power Doppler mode with a medium line density and a pulse repetition frequency of 9.3 kHz. The probe position relative to the chest wall was adjusted so that the mid-left ventricular (LV) cavity was at the acoustic focus (3 cm). The pulsing interval was adjusted to every 5 seconds. Cavitation was performed at a displayed mechanical index (MI) of 1.3. A suspension of 2×10^7 MBs in approximately 200 ml was administered intravenously over 30 seconds. US was continued for 10 minutes after initiation of the MB injection.

For cavitation in NHPs, a phased-array transducer interfaced with an US system (SONOS 7500) was positioned in an apical 4-chamber view. Power-harmonic Doppler imaging was performed at a pulsing interval of 5 seconds and the acoustic focus was placed at two-thirds the distance between the LV apex and mitral annular plane. MI was set at 1.3. Because of a more rapid blood pool clearance of MBs in NHPs compared to mice, a continuous infusion

of MBs was performed by administering 0.9 to 1.0 mL of Definity diluted in of saline over 8 minutes. US was performed for a duration of approximately 10 minutes.

Myocardial Perfusion Imaging Protocols

For both murine and NHP models, changes in myocardial perfusion produced by therapeutic cavitation was assessed with MCE protocols that minimize high-power MB cavitation. In wild-type (n=7) and Panx1$^{-/-}$ (n=5) mice, MCE was performed before cavitation, and again at 2–5 and 30 min after therapeutic cavitation. In wild-type mice, sham experiments were performed whereby MCE perfusion imaging was performed at similar time intervals (n=4). A linear-array transducer coupled to an US system (Sequoia 512, Siemens, Mountain View, CA) was positioned in a parasternal short-axis orientation to image the mid-ventricular plane. Low-power (MI 0.18) contrast-specific phase-inversion and amplitude-modulation technique was used at a transmission frequency of 7.0 MHz, and a dynamic range of 55 dB. Lipid-shelled decafluorobutane MBs were infused intravenously at a rate of 5×10^6 min^{-1}. Burst-replenishment imaging was performed by nulling MBs with 5 rapid frames at a MI of 0.98 followed by low-power acquisition of end-systolic frames by gating to the electrocardiogram.

In NHPs (n=8), MCE perfusion imaging was performed before therapeutic cavitation, within 5 min of completing cavitation, and 10 minutes later during maximal hyperemia produced by intravenous adenosine (140 μg/Kg/min) to determine residual hyperemic reserve. Perfusion was assessed in both the apical 4-chamber view (isoplanar with therapeutic cavitation) and in the 2-chamber view (control tissue). One vial of Definity MBs was diluted to a total volume of 30 mL and infused at 1.5 ml/min. Imaging was performed with a phased-array S3 transducer coupled to a Sonos 7500 US system. Intermittent ultraharmonic imaging (carrier frequency 1.6 MHz) triggered to end-systole was performed at a MI of 1.5. Gain values and compression were kept constant. Images were acquired during progressive prolongation of the pulsing interval from 1 to 8 cycles.

Regions-of-interest were drawn over the anterior wall in mice (to avoid issues with posterior attenuation), while in NHPs regions-of-interest were drawn over the septum in the apical 4-chamber view and the anterior wall in the apical 2-chamber view, excluding the apex which is shared between the two views. Background-subtracted time-intensity curves were fit to the function $y = A(1\text{-}e^{-\beta t})$, as previously described, where y represents video intensity at time t, A is the plateau intensity representing relative microvascular blood volume, and the rate constant β represents microvascular flux rate.[15] Myocardial blood flow was quantified by the product of A and β.[15]

Imaging of ATP-Release

Optical imaging methods to assess ATP release in vivo are provided in the Supplement.

Histology

Histology was performed on myocardial samples collected from the center of the cavitation zone 24 hours after therapeutic cavitation. Blood was cleared from the circulation using

isothermic PBS flush, and the heart was perfusion-fixed. Sections were stained with hematoxylin and eosin.

Cavitation Detection

Passive cavitation detection (PCD) was performed in an *ex vivo* heart model to confirm inertial cavitation of MBs. The methods are described in the online Supplement.

Statistical Analysis:

Data were analyzed with Prism v.7.0a (Graph Pad, La Jolla, CA). Tests for non-normal distribution were performed with the D'Agostino and Pearson omnibus test. For normally distributed data, one-way ANOVA was performed when multiple comparisons were made and a Student's *t*-test was used (paired or unpaired) for individual comparisons. For non-normally distributed data, a Kruskal-Wallis test was used followed by Mann-Whitney *U* test or Wilcoxon signed-rank test for individual comparisons. Time-dependent changes were assessed by repeated measures ANOVA. A Dunn's test or Holm-Sidak's multiple comparisons correction was used for multiple comparisons. Differences were considered significant at $p<0.05$.

RESULTS

Cavitation-mediated Myocardial Flow Augmentation in Mice

In mice undergoing MB cavitation at an MI of 1.3, MCE perfusion imaging was performed at 2–5 minutes and 30 minutes after cavitation based on recognition of two separate pathways for flow augmentation involving immediate ATP release from microporation, and sustained channel-mediated ATP release. In wild-type mice, post-cavitation myocardial perfusion increased significantly (64±25% vs baseline) when measured early after cavitation and increased further (95±55% vs baseline) when measured at 30 minutes (Figure 2A and Figure 3). On parametric analysis, flow augmentation at both post-cavitation time intervals was attributable mostly to an increase in microvascular flux rate (β-value) (Figure 2B and 2C). In Panx1$^{-/-}$ mice, myocardial perfusion was similar to wild-type mice at baseline and early after cavitation. However, Panx1$^{-/-}$ mice lacked the sustained flow augmentation response, with a return of perfusion to baseline values by 30 minutes. Differences in blood flow between the two mouse strains or between the study intervals were not secondary to any major differences in heart rate, a determinant of metabolic demand, (Supplemental Figure 1). In control sham-treated wild-type mice, myocardial perfusion remained constant (Figure 1D to 1F), indicating that neither procedure time nor MCE perfusion imaging influenced the post-cavitation changes in perfusion seen in the other treatment groups.

Myocardial ATP Generation and Histology

In vivo optical imaging in mice with a luciferin-luciferase reporter system detected a high level of ATP production that was localized to the site of transthoracic US-mediated MB cavitation (Figure 4A). A time-dependent decrease in luminescent signal was observed which is at least partially attributable to exhaustion of luciferin substrate rather than changes in ATP concentration. *Ex vivo* imaging of the chest organs indicated that most of the ATP signal originated from the heart (Figure 4B). On quantitative analysis (Figure 5), myocardial

ATP generation early after cavitation was an order of magnitude greater in wild-type than Panx1$^{-/-}$ mice (32.1±13.2 vs 3.5±1.5 ×10^5 p/s/cm^2), although signal in the Panx1$^{-/-}$ mice was still greater than 10-fold higher than sham-treated wild-type mice not undergoing cavitation (1.1±0.2 ×10^4 p/s/cm^2) ($p<0.05$). A time-dependent post-cavitation decay in ATP signal was seen in both wild-type and Panx1$^{-/-}$ mice. By 30 minutes, ATP signal in Panx1$^{-/-}$ mice had decreased to levels similar to sham-treated wild-type mice whereas wild-type mice continued to have a >100-fold higher ATP signal ($p<0.01$).

On histology, the appearance of the anterior myocardium one day after MB cavitation was similar to that of sham-treated control animals (Supplemental Figure 2). Notably, there was no evidence for petechial hemorrhage, inflammatory cell infiltrate, myocellular edema, or myocyte necrosis.

Cavitation-mediated Myocardial Flow Augmentation in Primates

In rhesus macaques, myocardial MB cavitation (MI 1.3) was well-tolerated without significant changes in vital signs, pulse oximetry, end-tidal CO_2 or cardiac rhythm. Table 1 illustrates the physiologic measurements, including parameters that influence myocardial oxygen demand, that were made at the time of each MCE perfusion imaging acquisition. Heart rate, systolic blood pressure, and double product all tended to be higher during adenosine than other stages, although these differences were small. After MB cavitation for 10 minutes performed only in the apical 4-chamber imaging plane, myocardial blood flow and flux rate increased in regions within the 4-chamber plane whereas no significant changes were seen in the apical 2-chamber plane (Figure 6). The degree of post-cavitation hyperemia in the apical 4-chamber plane was similar to that achieved during subsequent administration of intravenous adenosine performed to assess further hyperemic reserve. The degree of flow augmentation after cavitation was independent of the post-cavitation double product (Figure 7).

Cavitation Response

PCD in *ex vivo* pig hearts was performed to confirm that MBs were undergoing inertial cavitation (Supplemental Figure 3). PCD data were acquired with US applied at an MI of 0.6 and 1.3 in order to investigate MB response at the low- and high-end of the US pressures possible in the *in vivo* experiments based on attenuation coefficients up to 1 db/cm/MHz.[16] Although PCD response was pressure-dependent, at both MIs, frequency-amplitude spectra revealed peaks at the fundamental (1.3 MHz) and harmonic frequencies, and also the presence of strong broad-band (between-harmonic) signals, indicative of MB inertial cavitation.

DISCUSSION

Ultrasound has been used for a wide variety of therapeutic applications based on its ability to produce thermal and non-thermal bioeffects. Shear-mediated bioeffects within the vascular compartment are potentiated by the presence of MB contrast agents,[10,13] which are intravascular gas-filled bodies that undergo inertial cavitation or US-mediated destruction. In this study, we focused on changes in myocardial perfusion produced by MB cavitation, and

the mechanism underlying these changes. Our results indicate that substantial increases in flow are possible in mice, and in NHPs that are similar in microvascular physiology and endothelial biology to humans.[17] Gene-modified murine models were used to show that several pathways are involved in US-mediated release of ATP, a critically-important compound for flow augmentation after cavitation. Our results indicated that sustained flow augmentation in mice is mediated largely by shear-activated Panx-1 ATP channels.

There are many potential clinical benefits for creating focally high shear events in the myocardial microcirculation through US-mediated MB cavitation, including augmentation in perfusion, sonothrombolysis, and facilitated delivery of drugs or genes. In patients with myocardial infarction, high-MI exposure of MBs performed before and after primary percutaneous coronary intervention (PCI) has been shown to reduce infarct size.[12] In this setting, MB cavitation was intended to accelerate the lysis of arterial thrombus pre-PCI, yet benefit in terms of infarct size reduction and improvement in myocardial perfusion occurred even in those who did not achieve infarct-related artery patency prior to PCI. There are many potential explanations for this finding, reviewed elsewhere.[18] Benefit from direct microvascular vasodilation is likely based on previous studies demonstrating that MB cavitation can: (i) substantially increase limb or other msucle perfusion in mice, hamsters, and humans (including those with peripheral artery disease);[10,11,19,20] (ii) reverse limb ischemia in mice,[10,11] and (iii) increase limb perfusion in patients with sickle cell disease.[11]

Our findings firmly establish that brief (10 minute) MB cavitation with US parameters approved for use in humans and MB doses scaled to human equivalency, substantially increases myocardial perfusion in mice and NHPs. In C57 mice, flow reserve is low (approximately 2.5-fold), in part because of high resting perfusion.[21] Accordingly, we believe the degree of flow augmentation in mice 30 minutes after cavitation was near maximal.[3] In rhesus macaques, we believe that MB cavitation produced near-maximal flow based on comparisons to measurement of residual vasodilator reserve with adenosine. Similar to mice, flow reserve in rhesus macaques is lower than in humans due, in part, to faster basal heart rates and contractile states that require higher baseline flow. In the NHPs, flow augmentation occurred only in myocardial territories exposed to cavitation energy (4-chamber plane) with minimal change in the remote (2-chamber) territory. Previous studies of cavitation in the murine hindlimb have revealed flow augmentation extending well beyond the region of cavitation.[11] This finding was thought to reflected conducted vasodilation from downstream effects from ATP released in blood, or from vascular network signaling.[22] Neither of these mechanisms would be predicted to occur in remote myocardium (e.g. 2-chamber plane) after exposure of the 4-chember plane since they do not share a microvascular network.

Previous studies performed in the coronary and peripheral vasculature have implicated shear-mediated pathways, NO release in particular, in the US-mediated vasodilation and flow augmentation that occurs with or without MB cavitation.[9,10,14,23] Recent studies have provided even greater mechanistic detail. In the peripheral circulation, cavitation causes immediate release of ATP from both endothelial and RBC sources.[11] Vasodilation then occurs from endothelial signaling (through P2Y- and A2b-receptors) of NO and prostaglandin production, and from ectonucleotidase conversion of ATP to adenosine which

acts on smooth muscle cell A2a receptors. While immediate ATP release in these studies could be attributed to transient microporation of cells; there was also sustained release of ATP and flow augmentation in ischemic tissues that persisted for over 24 hours, and that could not be attributed to microporation.[11] This sustained response is likely to represent activation of shear-mediated ATP channels, of which Panx1 appears to be important (unpublished data).

The current study is the first to investigate ATP release after MB cavitation in the coronary circulation. In wild-type mice, myocardial ATP release was several orders of magnitude greater in mice undergoing cavitation than in controls. Augmentation in flow was primarily manifest as an increase in microvascular flux rate (β), which is consistent with an arteriolar level of action where purinergic vasodilation is operative.[3] In mice lacking the Panx1$^{-/-}$ channel, while there was evidence for myocardial ATP release early after cavitation that was associated with an increase in microvascular perfusion, the degree of ATP release was blunted compared to wild-type mice. These findings indicate that immediate post-cavitation ATP response involves Panx1, but in combination with other pathways, such as microporation and perhaps other ATP release mechanisms.[24] The defect in flow augmentation early after cavitation in Panx1$^{-/-}$ was small compared to the relative reduction in immediate ATP release, suggesting that there may be a point at which increasing release of ATP does not produce further increases in flow. The decrease of myocardial ATP to control levels and return of myocardial perfusion to baseline values at 30 minutes in Panx1$^{-/-}$ mice strongly suggests that sustained ATP release is mediated through Panx1 channels.

Our results have clinical implications for both acute and chronic ischemic conditions. Recent clinical trials have demonstrated that MB cavitation can reduce infarct size in patients with acute MI, even when epicardial recanalization doesn't occur.[12] There are many potential explanations for these findings, including ameliorative effects on reflow.[18] Our data suggests that the effects of cavitation of myocardial blood flow are likely to be important, and could be of benefit when given either before or after reperfusion. The identification of cavitation-related flow augmentation as a major mechanism for reducing ischemic injury would help guide protocols towards priority on microvascular rather than epicardial exposure. Acute flow augmentation could also be a potential means to reverse stress-related cardiomyopathies, a condition thought to be worsened by abnormal vascular tone. In chronic ischemic heart failure, cavitation could be of benefit in situations where temporary augmentation of flow is desired, such in periods of increased demand or in preparation of high-risk surgery. The finding that ATP is released in the myocardium with cavitation is also important since purinergic signaling can produce other beneficial effects than flow augmentation, such as anti-platelet, anti-inflammatory, and pro-angiogenic signaling.[25–27]

There are several limitations of this study that deserve mention. Measurement of absolute ATP concentration in the myocardium was not possible in these experiments, and time-dependent ATP changes were likely influenced by a reduction in luciferin substrate. Accordingly, the most robust comparisons involve temporal differences between mouse strains. We did not directly assess microporation as a mechanism for the early ATP release primarily because this mechanism has already been established.[11] In the NHP studies,

perfusion imaging was performed with intermittent high-MI. While this approach may have influenced flow, the degree was very small evidenced by data from the control 2-chamber plane. It is also worth noting that effects of cavitation may be influenced by the presence of hyperlipidemia or diabetes, both of which influence endothelial-derived pathways that mediate vasodilation in response to purines. Finally, we did not assess duration of myocardial flow response in NHPs primarily because of the need to complete both cavitation response and adenosine response in a timely manner in anesthetized animals. Moreover, the current studies were performed in non-ischemic tissue whereas our previous results in murine hindlimb ischemia models have indicated that the duration of flow response to cavitation is longer in ischemic than normal limbs.

In summary, our findings indicate that cavitation of MB contrast agents in the coronary microcirculation produces augmentation in myocardial perfusion that is immediate, sustained, and safe. Flow augmentation up to two-fold can be produced in primate models with a vascular physiology similar to that in humans. Sustained flow augmentation appears to be mediated largely through shear-mediated activation of ATP channels. These results have direct clinical impact by providing a mechanistic framework for studies showing a benefit of MB cavitation in patients with acute myocardial infarction; and for consideration of other potential applications of shear-mediated responses such as the stimulation of angiogenesis or reduction in vascular inflammatory response.

Supplementary Material

Refer to Web version on PubMed Central for supplementary material.

ACKNOWLEDGEMENTS

The authors of this manuscript would like to recognize the life and career of our collaborator and friend Sabine Huke who tragically passed away in 2018. She will be missed by many.

FUNDING SOURCES

Dr. Lindner is supported by grants R01-HL078610, R01-HL130046, and P51-OD011092 from the National Institutes of Health, Bethesda, MD. Dr. Lindner is also supported by a grant (14-14NSBRI1-0025) from the NASA National Space Biomedical Research Institute. Dr. Moccetti is supported by a grant from the Swiss National Science Foundation and Novartis Foundation for Biomedical Research. Mr. Brown is supported by grant 18PRE33960532 from the American Heart Association. Dr. Ozawa is supported by the JSPS Overseas Research Fellowship Foundation and a Manpei Suzuki Diabetes grant.

ABBREVIATIONS

CEU	Contrast-enhanced ultrasound
MB	Microbubble
MCE	Myocardial contrast echocardiography
MI	Mechanical index
NHP	Nonhuman Primate
NO	Nitric oxide

Panx1	Pannexin-1
RBC	Red blood cells

REFERENCES

1. Feigl EO. Coronary physiology. Physiol Rev. 1983;63:1–205. [PubMed: 6296890]
2. Marcus ML, Chilian WM, Kanatsuka H, Dellsperger KC, Eastham CL and Lamping KG. Understanding the coronary circulation through studies at the microvascular level. Circulation. 1990;82:1–7. [PubMed: 2114232]
3. Durand MJ and Gutterman DD. Diversity in mechanisms of endothelium-dependent vasodilation in health and disease. Microcirculation. 2013;20:239–47. [PubMed: 23311975]
4. Forsyth AM, Wan J, Owrutsky PD, Abkarian M and Stone HA. Multiscale approach to link red blood cell dynamics, shear viscosity, and ATP release. Proc Natl Acad Sci USA. 2011;108:10986–91. [PubMed: 21690355]
5. Wan J, Ristenpart WD and Stone HA. Dynamics of shear-induced ATP release from red blood cells. Proc Natl Acad Sci USA. 2008;105:16432–7. [PubMed: 18922780]
6. Locovei S, Bao L and Dahl G. Pannexin 1 in erythrocytes: function without a gap. Proc Natl Acad Sci USA. 2006;103:7655–9. [PubMed: 16682648]
7. Cinar E, Zhou S, DeCourcey J, Wang Y, Waugh RE and Wan J. Piezo1 regulates mechanotransductive release of ATP from human RBCs. Proc Natl Acad Sci USA. 2015;112:11783–8. [PubMed: 26351678]
8. Iida K, Luo H, Hagisawa K, Akima T, Shah PK, Naqvi TZ, et al. Noninvasive low-frequency ultrasound energy causes vasodilation in humans. J Am Coll Cardiol. 2006;48:532–7. [PubMed: 16875980]
9. Suchkova VN, Baggs RB, Sahni SK and Francis CW. Ultrasound improves tissue perfusion in ischemic tissue through a nitric oxide dependent mechanism. Thromb Haemost. 2002;88:865–70. [PubMed: 12428107]
10. Belcik JT, Mott BH, Xie A, Zhao Y, Kim S, Lindner NJ, et al. Augmentation of limb perfusion and reversal of tissue ischemia produced by ultrasound-mediated microbubble cavitation. Circ Cardiovasc Imaging. 2015;8:e002979. [PubMed: 25834183]
11. Belcik JT, Davidson BP, Xie A, Wu MD, Yadava M, Qi Y, et al. Augmentation of Muscle Blood Flow by Ultrasound Cavitation Is Mediated by ATP and Purinergic Signaling. Circulation. 2017;135:1240–1252. [PubMed: 28174191]
12. Mathias W Jr., Tsutsui JM, Tavares BG, Fava AM, Aguiar MOD, Borges BC, et al. Sonothrombolysis in ST-Segment Elevation Myocardial Infarction Treated With Primary Percutaneous Coronary Intervention. J Am Coll Cardiol. 2019;73:2832–2842. [PubMed: 30894317]
13. Xie F, Lof J, Matsunaga T, Zutshi R and Porter TR. Diagnostic ultrasound combined with glycoprotein IIb/IIIa-targeted microbubbles improves microvascular recovery after acute coronary thrombotic occlusions. Circulation. 2009;119:1378–85. [PubMed: 19255341]
14. Siegel RJ, Suchkova VN, Miyamoto T, Luo H, Baggs RB, Neuman Y, et al. Ultrasound energy improves myocardial perfusion in the presence of coronary occlusion. J Am Coll Cardiol. 2004;44:1454–8. [PubMed: 15464327]
15. Wei K, Jayaweera AR, Firoozan S, Linka A, Skyba DM and Kaul S. Quantification of myocardial blood flow with ultrasound-induced destruction of microbubbles administered as a constant venous infusion. Circulation. 1998;97:473–83. [PubMed: 9490243]
16. O'Brien WD Jr., Yang Y, Simpson DG, Frizzell LA, Miller RJ, Blue JP Jr., et al. Threshold estimation of ultrasound-induced lung hemorrhage in adult rabbits and comparison of thresholds in mice, rats, rabbits and pigs. Ultrasound Med Biol. 2006;32:1793–804. [PubMed: 17112965]
17. Cox LA, Olivier M, Spradling-Reeves K, Karere GM, Comuzzie AG and VandeBerg JL. Nonhuman Primates and Translational Research-Cardiovascular Disease. ILAR J. 2017;58:235–250. [PubMed: 28985395]

18. Lindner JR. Therapeutic Contrast Echocardiography: Bubbles Become Medicine. J Am Coll Cardiol. 2019;73:2843–2845. [PubMed: 31171089]
19. Mason OR, Davidson BP, Sheeran P, Muller M, Hodovan JM, Sutton J, et al. Augmentation of Tissue Perfusion in Patients With Peripheral Artery Disease Using Microbubble Cavitation. JACC Cardiovasc Imaging. 2019.
20. Bertuglia S Increase in capillary perfusion following low-intensity ultrasound and microbubbles during postischemic reperfusion. Crit Care Med. 2005;33:2061–7. [PubMed: 16148481]
21. Raher MJ, Thibault H, Poh KK, Liu R, Halpern EF, Derumeaux G, et al. In vivo characterization of murine myocardial perfusion with myocardial contrast echocardiography: validation and application in nitric oxide synthase 3 deficient mice. Circulation. 2007;116:1250–7. [PubMed: 17709634]
22. Bagher P and Segal SS. Regulation of blood flow in the microcirculation: role of conducted vasodilation. Acta Physiol (Oxf). 2011;202:271–84. [PubMed: 21199397]
23. Atar S, Siegel RJ, Akel R, Ye Y, Lin Y, Modi SA, et al. Ultrasound at 27 kHz increases tissue expression and activity of nitric oxide synthases in acute limb ischemia in rabbits. Ultrasound Med Biol. 2007;33:1483–8. [PubMed: 17507145]
24. Burnstock G and Verkhratsky A. Mechanisms of ATP release and inactivation In: Burnstock G and Verkhratsky A, eds. Purinergic Signalling and the Nervous System. 1st ed. Berlin, Germany: Springer-Verlag; 2012: 79–118.
25. Rumjahn SM, Yokdang N, Baldwin KA, Thai J and Buxton IL. Purinergic regulation of vascular endothelial growth factor signaling in angiogenesis. Br J Cancer. 2009;100:1465–70. [PubMed: 19367276]
26. Cekic C and Linden J. Purinergic regulation of the immune system. Nat Rev Immunol. 2016;16:177–92. [PubMed: 26922909]
27. Johnston-Cox HA and Ravid K. Adenosine and blood platelets. Purinergic Signal. 2011;7:357–65. [PubMed: 21484090]

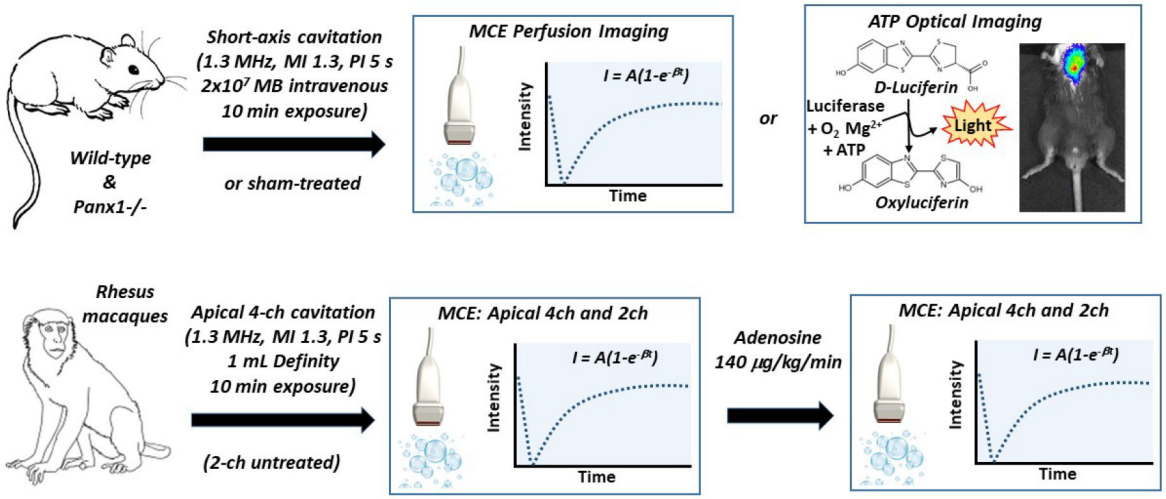

Figure 1.
Schematic of study design. MB, microbubble; Panx1−/−, pannexin-1 channel deficient mice.

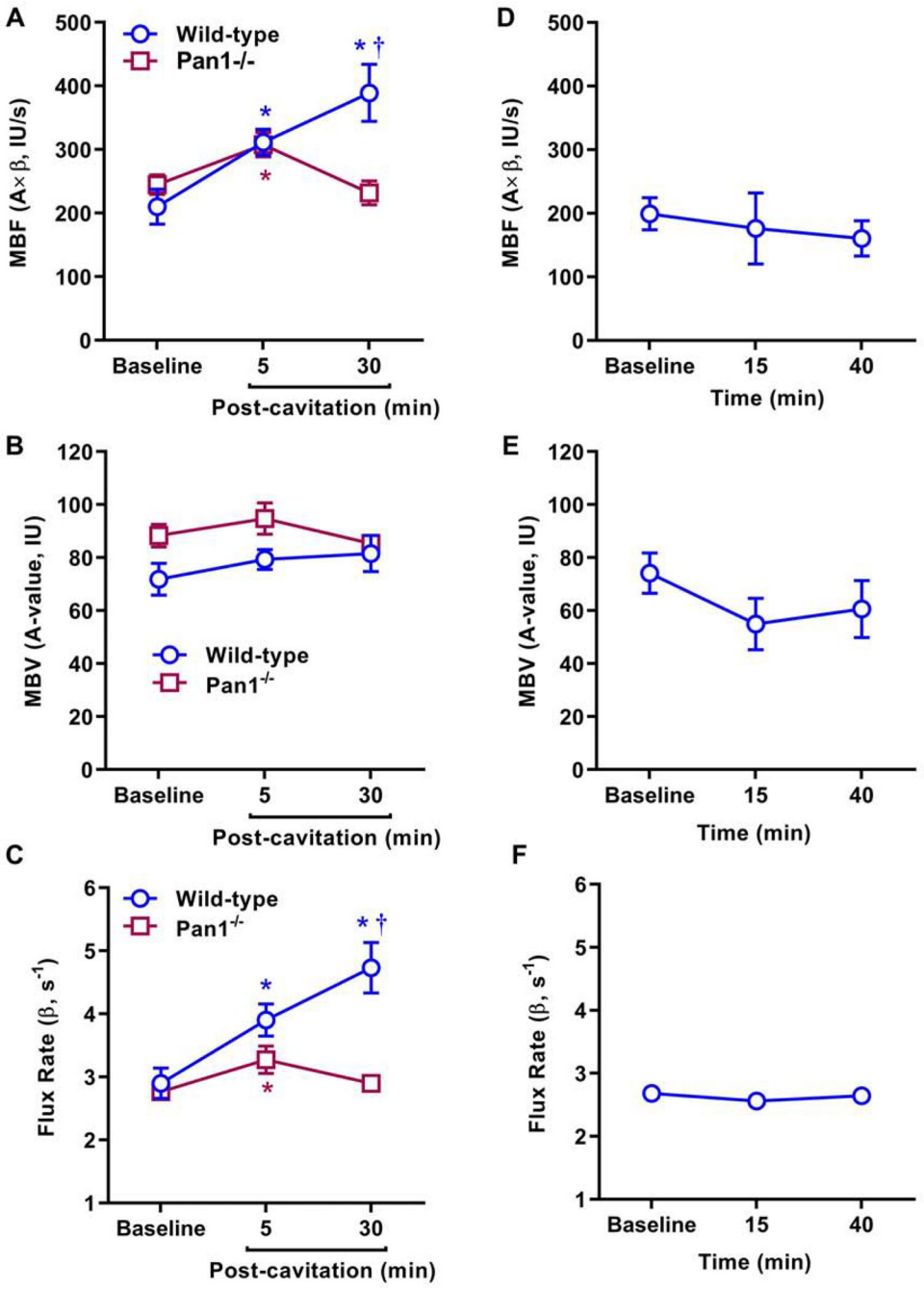

Figure 2.

Mean (±SEM) values for MCE-derived microvascular blood flow (*MBF*, A×β), microvascular blood volume (*MBV*, A-value), and microvascular flux rate (β) in wild-type and Panx1$^{-/-}$ mice undergoing MB cavitation (**A** to **C**); and sham-treated wild-type mice (**D** to **F**). *p<0.05 versus baseline; †p<0.05 versus Panx1$^{-/-}$.

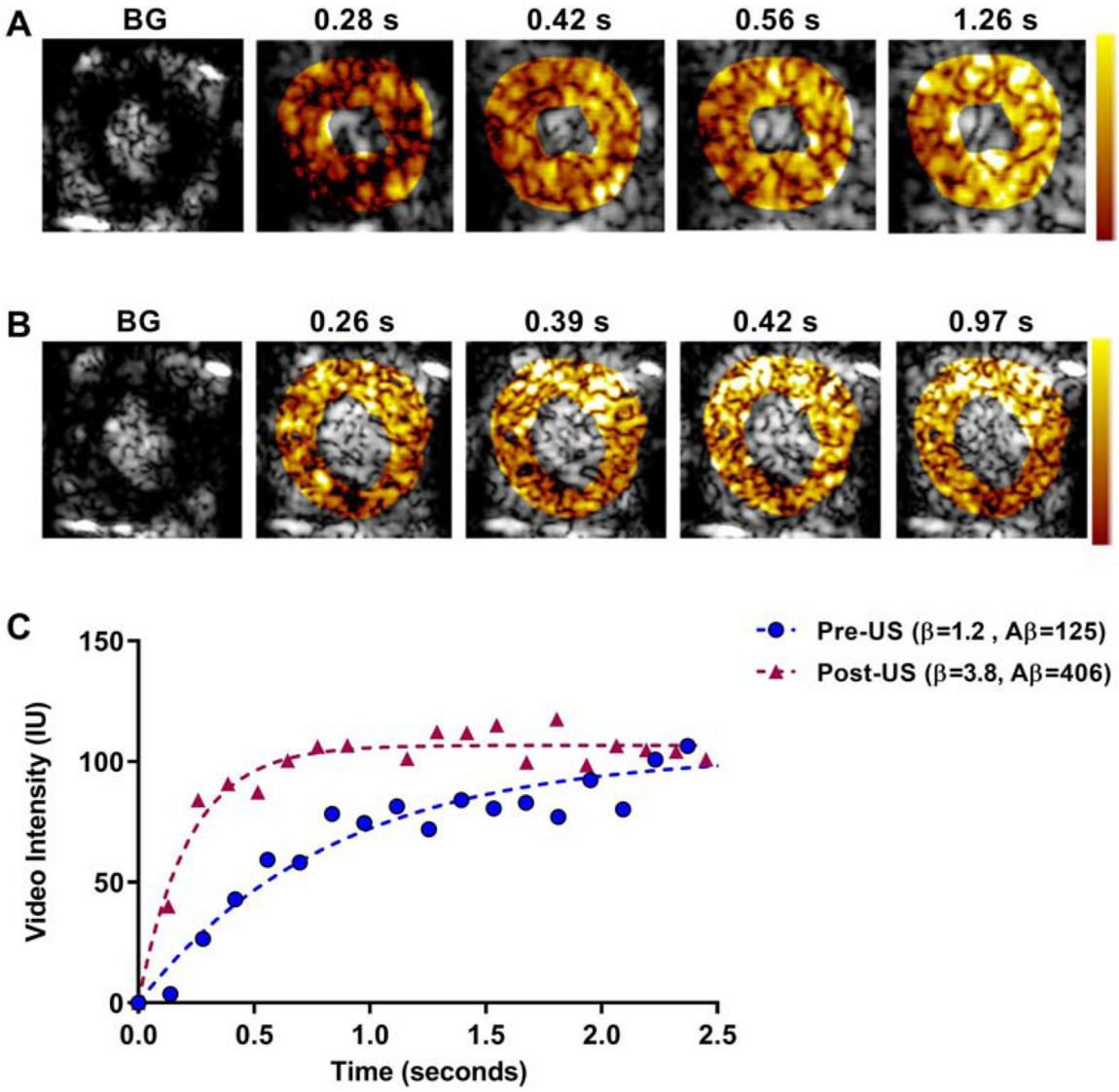

Figure 3.

Examples of background-subtracted color-coded (scale at left) MCE perfusion images with increasing time in seconds (s) after MB destruction from a mouse at (A) baseline and (**B**) 30 minutes after therapeutic cavitation. (**B**) MCE time-intensity curves after microbubble destruction from a mouse at baseline and 30 minutes after therapeutic cavitation. The baseline data correlate to images shown in panel A.

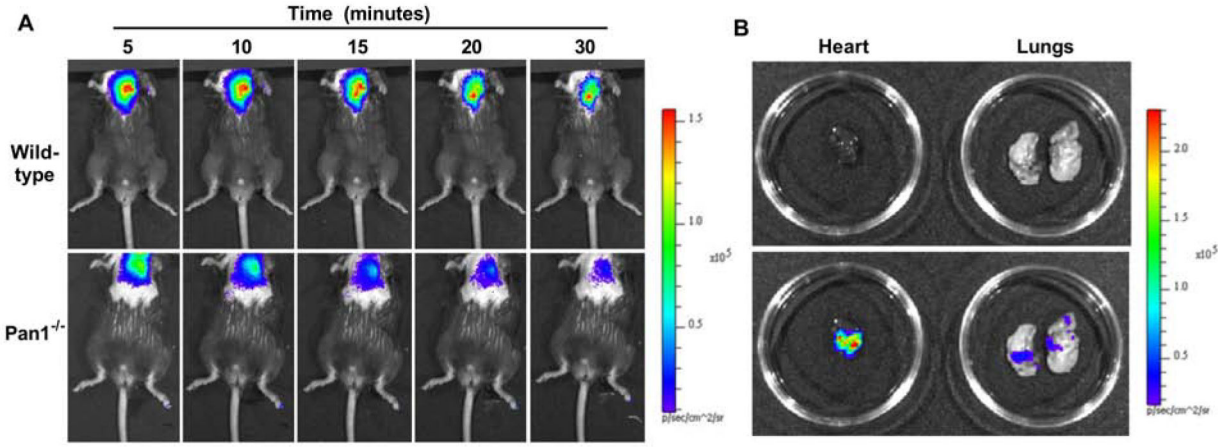

Figure 4. (A)

Examples of *in vivo* optical imaging of ATP production using a luciferin-luciferase assay in anesthetized wild-type and Panx1$^{-/-}$ mice at increasing time intervals after MB cavitation. **(B)** Examples of *ex vivo* imaging using bright light without (top) and with (bottom) superimposed luminescence imaging for the lung and heart from a wild-type mouse undergoing myocardial MB cavitation. Scales are shown to the right.

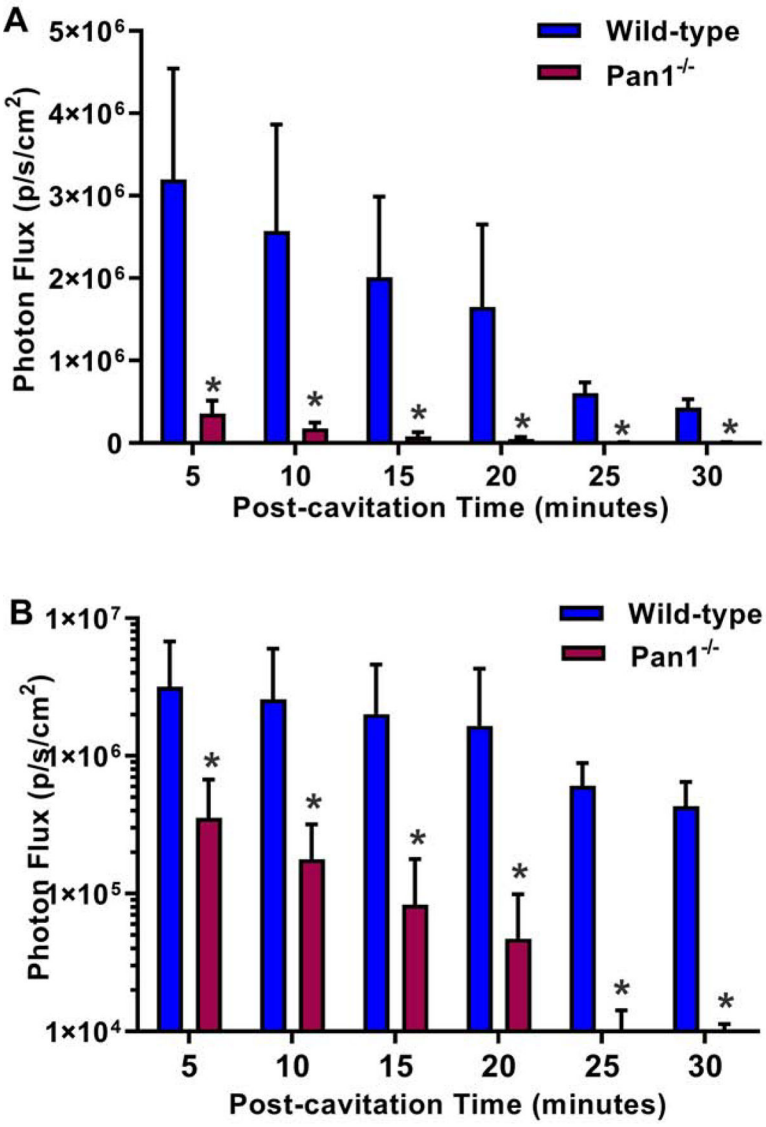

Figure 5.

Mean (±SEM) photon flux on optical imaging of ATP activity from regions-of-interest placed over the anterior chest after ultrasound cavitation in wild-type and Panx1$^{-/-}$ mice. Data are displayed with optical imaging data in linear (**A**), and log-compressed (**B**) scale. *p<0.05 versus Panx1$^{-/-}$.

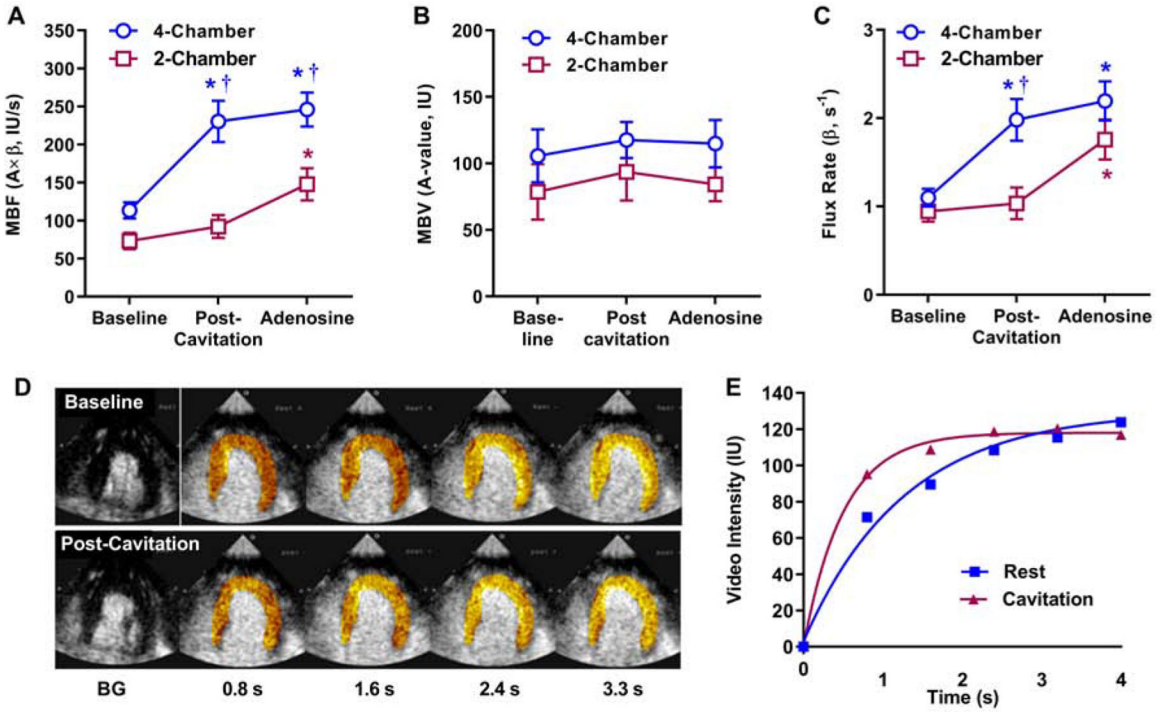

Figure 6.

Mean (±SEM) values for MCE-derived (**A**) microvascular blood flow (*MBF*, A×β), (B) microvascular blood volume (*MBV*, A-value), and (**C**) microvascular flux rate (β) in rhesus macaques. Data are shown for resting conditions, post-cavitation (performed only in tissue within the apical 4-chamber plane), and adenosine infusion). *p<0.05 versus baseline; †p<0.05 versus 2-chamber data. (**D** and **E**) Background-subtracted color-coded images and corresponding time-intensity data from the apical 4 chamber view illustrating increase in myocardial perfusion by cavitation.

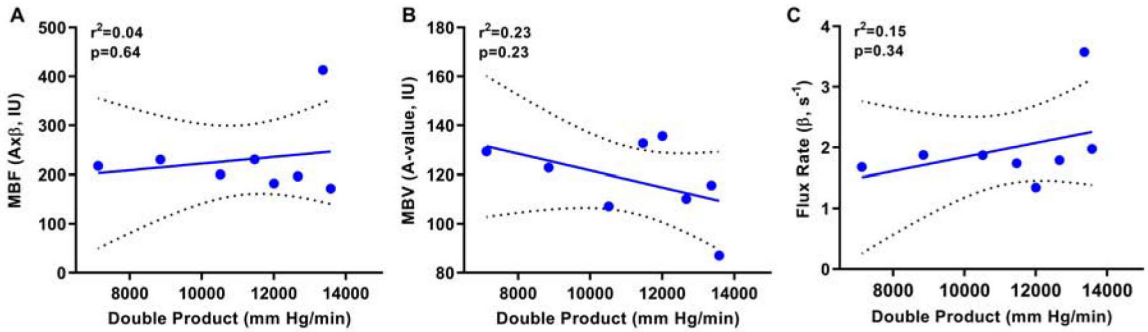

Figure 7.

Relations between double product in NHPs at the time of post-cavitation imaging and the perfusion parameters on MCE including (**A**) microvascular blood flow, (**B**) microvascular blood volume (*A-value*), and (**C**) microvascular flux rate (*β-value*). Solid line=line of identity; dashed line=standard error of the estimate.

Table 1.

Vital Signs Measured During Non-human Primate Studies

	Baseline	Cavitation	Adenosine
Heart Rate (min^{-1})	130±15	128±13	134±12
Systolic BP (mm Hg)	84± 13	87±14	91±13*
Diastolic BP (mm Hg)	40±9	42±8	41±11
Double Product (mm Hg min^{-1})	10,951±2,271	11,196±2,264	12,195±2,154*
O_2 Saturation (%)	96±1	95±2	95±2
End-tidal CO_2 (mm Hg)	41±8	41±17	41±7

* $p<0.05$ versus Baseline.